Three-dimensional dielectric crystalline waveguide beam splitters in mid-infrared band by direct femtosecond laser writing

Ruiyun He,[1] Irene Hernández-Palmero,[2] Carolina Romero,[2] Javier R. Vázquez de Aldana,[3] and Feng Chen[1,*]

[1]*School of Physics, State Key Laboratory of Crystal Materials, Shandong University, Jinan 250100, China*
[2]*Centro de Láseres Pulsados (CLPU), Parque Científico, 37185 Villamayor, Salamanca, Spain*
[3]*Laser Microprocessing Group, Universidad de Salamanca, Salamanca 37008, Spain*
[*]*drfchen@sdu.edu.cn*

Abstract: We report on the fabrication of three-dimensional waveguide beam splitters in a dielectric $Bi_4Ge_3O_{12}$ (BGO) crystal by direct femtosecond laser writing. In the laser written tracks of BGO crystal, positive refractive index is induced, resulting in so-called Type I configuration waveguiding cores. The "multiscan" technique is utilized to shape cores with designed cross-sectional geometry in order to achieve guidance at mid-infrared wavelength of 4 μm. The fundamental mode guidance along both TE and TM polarizations has been obtained in the waveguide structures. With this feature, we implement beam splitters from 2D to 3D geometries, and realize 1 × 2, 1 × 3, and 1 × 4 power splitting at 4μm.

OCIS codes: (140.3390) Laser materials processing; (230.7370) Waveguides; (230.1360) Beam splitters; (130.3060) Infrared.

References and links

1. E. J. Murphy, *Integrated Optical Circuits and Components: Design and Applications* (Marcel Dekker, 1999).
2. G. C. Righini and A. Chiappini, "Glass optical waveguides: a review of fabrication techniques," Opt. Eng. **53**(7), 071819 (2014).
3. M. Quintanilla, E. M. Rodríguez, E. Cantelar, F. Cussó, and C. Domingo, "Micro-Raman characterization of Zn-diffused channel waveguides in Tm^{3+}:$LiNbO_3$," Opt. Express **18**(6), 5449–5458 (2010).
4. A. Tervonen, B. R. West, and S. Honkanen, "Ion-exchanged glass waveguide technology: a review," Opt. Eng. **50**(7), 071107 (2011).
5. F. Chen, "Micro-and submicrometric waveguiding structures in optical crystals produced by ion beams for photonic applications," Laser Photon. Rev. **6**(5), 622–640 (2012).
6. R. W. Eason, T. C. May-Smith, C. Grivas, M. S. B. Darby, D. P. Shepherd, and R. Gazia, "Current state-of-the-art of pulsed laser deposition of optical waveguide structures: Existing capabilities and future trends," Appl. Surf. Sci. **255**(10), 5199–5205 (2009).
7. F. Chen and J. R. Vazquez de Aldana, "Optical waveguides in crystalline dielectric materials produced by femtosecond-laser micromachining," Laser Photon. Rev. **8**(2), 251–275 (2014).
8. D. Choudhury, J. R. Macdonald, and A. K. Kar, "Ultrafast laser inscription: perspectives on future integrated applications," Laser Photonics Rev. **8**(6), 827–846 (2014).
9. T. Calmano and S. Müller, "Crystalline waveguide lasers in the visible and near-infrared spectral range," IEEE J. Sel. Top. Quantum Electron. **21**(1), 1602213 (2015).
10. K. Song, Y. Fan, and Y. H. Zhang, "Broad-band power divider based on radial waveguide," Microw. Opt. Technol. Lett. **49**(3), 595–597 (2007).
11. M. Sakakura, T. Sawano, Y. Shimotsuma, K. Miura, and K. Hirao, "Fabrication of three-dimensional 1 x 4 splitter waveguides inside a glass substrate with spatially phase modulated laser beam," Opt. Express **18**(12), 12136–12143 (2010).
12. S. Nolte, M. Will, J. Burghoff, and A. Tuennermann, "Femtosecond waveguide writing: a new avenue to three-dimensional integrated optics," Appl. Phys., A Mater. Sci. Process. **77**(1), 109–111 (2003).
13. Y. Tan, F. Chen, X. L. Wang, L. Wang, V. M. Shandarov, and D. Kip, "Formation of reconfigurable optical channel waveguides and beam splitters on top of proton-implanted lithium niobate crystals using spatial dark soliton-like structures," J. Phys. D Appl. Phys. **41**(10), 102001 (2008).
14. R. R. Gattass and E. Mazur, "Femtosecond laser micromachining in transparent materials," Nat. Photonics **2**(4), 219–225 (2008).

#226064 - $15.00 USD Received 30 Oct 2014; revised 27 Nov 2014; accepted 28 Nov 2014; published 10 Dec 2014

15. M. Ams, G. D. Marshall, P. Dekker, J. A. Piper, and M. J. Withford, "Ultrafast laser written active devices," Laser Photon. Rev. **3**(6), 535–544 (2009).
16. K. Sugioka and Y. Cheng, "Ultrafast lasers: reliable tools for advanced materials processing," Light Sci. Appl. **3**(4), e149 (2014).
17. Y. Liao, J. Song, E. Li, Y. Luo, Y. Shen, D. Chen, Y. Cheng, Z. Xu, K. Sugioka, and K. Midorikawa, "Rapid prototyping of three-dimensional microfluidic mixers in glass by femtosecond laser direct writing," Lab Chip **12**(4), 746–749 (2012).
18. N. Pavel, G. Salamu, F. Jipa, and M. Zamfirescu, "Diode-laser pumping into the emitting level for efficient lasing of depressed cladding waveguides realized in Nd:YVO_4 by the direct femtosecond-laser writing technique," Opt. Express **22**(19), 23057–23065 (2014).
19. G. Salamu, F. Jipa, M. Zamfirescu, and N. Pavel, "Cladding waveguides realized in Nd:YAG ceramic by direct femtosecond-laser writing with a helical movement technique," Opt. Mater. Express **4**(4), 790–797 (2014).
20. A. Zoubir, C. Lopez, M. Richardson, and K. Richardson, "Femtosecond laser fabrication of tubular waveguides in poly(methyl methacrylate)," Opt. Lett. **29**(16), 1840–1842 (2004).
21. R. Osellame, M. Lobino, N. Chiodo, M. Marangoni, G. Cerullo, R. Ramponi, H. T. Bookey, R. R. Thomson, N. D. Psaila, and A. K. Kar, "Femtosecond laser writing of waveguides in periodically poled lithium niobate preserving the nonlinear coefficient," Appl. Phys. Lett. **90**(24), 241107 (2007).
22. A. Rodenas and A. K. Kar, "High-contrast step-index waveguides in borate nonlinear laser crystals by 3D laser writing," Opt. Express **19**(18), 17820–17833 (2011).
23. R. Y. He, Q. An, J. R. Vázquez de Aldana, Q. M. Lu, and F. Chen, "Femtosecond-laser micromachined optical waveguides in $Bi_4Ge_3O_{12}$ crystals," Appl. Opt. **52**(16), 3713–3718 (2013).
24. A. Ródenas, G. Martin, B. Arezki, N. Psaila, G. Jose, A. Jha, L. Labadie, P. Kern, A. Kar, and R. Thomson, "Three-dimensional mid-infrared photonic circuits in chalcogenide glass," Opt. Lett. **37**(3), 392–394 (2012).
25. W. Drozdowski, A. J. Wojtowicz, S. M. Kaczmarek, and M. Berkowski, "Scintillation yield of $Bi_4Ge_3O_{12}$ (BGO) pixel crystals," Physica B **405**(6), 1647–1651 (2010).
26. J. Yang, C. Zhang, F. Chen, Sh. Akhmadaliev, and S. Q. Zhou, "Planar optical waveguides in $Bi_4Ge_3O_{12}$ crystal fabricated by swift heavy-ion irradiation," Appl. Opt. **50**(36), 6678–6681 (2011).
27. I. Bányász, S. Berneschi, N. Q. Khánh, T. Lohner, K. Lengyel, M. Fried, Á. Péter, P. Petrik, Z. Zolnai, A. Watterich, G. Nunzi-Conti, S. Pelli, and G. C. Righini, "Formation of slab waveguides in eulytine type BGO and CaF_2 crystals by implantation of MeV nitrogen ions," Nucl. Instr. Meth. B **286**, 80–84 (2012).
28. I. Bányász, Z. Zolnai, S. Pelli, S. Berneschid, M. Fried, T. Lohner, G. Nunzi-Conti, and G. C. Righini, "Single- and double-energy N^+ - irradiated planar waveguides in eulytine and sillenite type BGO crystals," Proc. SPIE **8627**, 862705 (2013).
29. I. Vurgaftman, J. R. Meyer, N. Tansu, and L. J. Mawst, "InP-Based Dilute-Nitride Mid-Infrared Type-II 'W' Quantum-Well Lasers," J. Appl. Phys. **96**(8), 4653–4655 (2004).
30. R. Y. He, Q. An, Y. C. Jia, G. R. Castillo-Vega, J. R. Vázquez de Aldana, and F. Chen, "Femtosecond laser micromachining of lithium niobate depressed cladding waveguides," Opt. Mater. Express **3**(9), 1378–1384 (2013).
31. Y. Y. Ren, G. Brown, A. Ródenas, S. Beecher, F. Chen, and A. K. Kar, "Mid-infrared waveguide lasers in rare-earth-doped YAG," Opt. Lett. **37**(16), 3339–3341 (2012).
32. A. J. Maker and A. M. Armani, "Low-loss silica-on-silicon waveguides," Opt. Lett. **36**(19), 3729–3731 (2011).
33. D. G. Lancaster, S. Gross, H. Ebendorff-Heidepriem, M. J. Withford, T. M. Monro, and S. D. Jackson, "Efficient 2.9 μm fluorozirconate glass waveguide chip laser," Opt. Lett. **38**(14), 2588–2591 (2013).
34. J. R. Macdonald, S. J. Beecher, A. Lancaster, P. A. Berry, K. L. Schepler, S. B. Mirov, and A. K. Kar, "Compact Cr:ZnS channel waveguide laser operating at 2,333 nm," Opt. Express **22**(6), 7052–7057 (2014).
35. J. R. Macdonald, S. J. Beecher, P. A. Berry, K. L. Schepler, and A. K. Kar, "Compact mid-infrared Cr:ZnSe channel waveguide laser," Appl. Phys. Lett. **102**(16), 161110 (2013).
36. J. Siebenmorgen, K. Petermann, G. Huber, K. Rademaker, S. Nolte, and A. Tunnermann, "Femtosecond laser written stress-induced Nd:$Y_3Al_5O_{12}$ (Nd:YAG) channel waveguide laser," Appl. Phys. B **97**(2), 251–255 (2009).
37. RSoft Design Group, Computer software BandSLOVE, *http://www.rsoftdesign.com*

1. Introduction

Optical waveguides, as the basic components in integrated photonics, offer the confinement of light propagation within small volumes, in which relatively high optical intensities could be achieved [1,2]. Several techniques, including metal-ion indiffusion [3], ion/proton exchange [4], ion implantation/irradiation [5], epitaxial layer deposition [6], and femtosecond laser micromachining/writing [7–9], have been employed to fabricate diverse configurations in various materials. Particularly, a number of approaches to achieving waveguide beam splitters, which could divide the input beam equally into multiple output waveguides without significant additional loss, have been reported in the literatures [10–13].

Recent years, the femtosecond laser writing has been widely applied as one of the most efficient techniques for micro-fabrication of transparent optical materials due to the advantageous capability of direct 3D micromachining over competing techniques [14–16]. In optics, it appears as a direct, rapid, maskless fabrication technique that can create optical

#226064 - $15.00 USD Received 30 Oct 2014; revised 27 Nov 2014; accepted 28 Nov 2014; published 10 Dec 2014

waveguides or more complicated photonic devices (splitters, optical circuits, etc.), avoiding temperature control or complex clean room facilities. With a suitable choice of laser parameters (wavelength, polarization, repetition rate, pulse energy, focusing conditions, moving speed), one can inscribe devices in various optical materials, including glass [11, 12, 17], crystals [18], ceramics [19], and polymers [20]. Femtosecond laser pulses with high intensities induce extremely localized modifications of material matrix through nonlinear absorption processes. The refractive index modification of the femtosecond laser irradiated regions could be either positive or negative, depending on the materials' nature as well as the laser parameters. The well-accepted configuration classification of femtosecond laser written optical waveguides includes Type I (index increased in the irradiated region) [7–9, 21, 22] and Type II (guiding cores typically within the region between two parallel damage tracks of reduced index) [7–9, 23], and Type III cladding structures (cores surrounded by a number of low-index tracks) [7–9]. Particularly, Type I structures are easier for direct 3D fabrication of complex devices. Moreover, the "multiscan" fabrication technique could be used to produce positive step-index cores with desirable cross-sectional shape [22, 24]. While it is very common in glasses [19, 20], Type I waveguides have only been reported in a few crystals, including LiNbO3 [21] and Nd:YCOB [22], with limitations in stability and polarization.

Bismuth germanate ($Bi_4Ge_3O_{12}$ or BGO) is a well-known scintillating crystal with cubic structure [25]. The features of BGO crystal, such as non-hygroscopic, high electro-optic coefficient and easy preparation, make it an ideal crystal for nuclear physics, space physics, high-energy physics, medicine, industry and other fields. In early works, BGO waveguides were fabricated by ion implantation/irradiation [26–28]. Femtosecond laser micromachining was also utilized in BGO crystal to fabricate Type II dual-line and depressed cladding waveguides [23]. Based on our previous work, we aim to write Type I BGO crystal waveguides supporting guidance along any transverse polarization. On the other hand, spurred by the development of quantum cascade lasers (QCLs) and fiber lasers [29], the MIR part of the spectra has become a region of numerous scientific and technological interests. So far, MIR optical waveguides have been reported in $LiNbO_3$ crystal [30], YAG crystal [31], silica on silicon [32], and chalcogenide glass [24], etc. The realization of compact MIR laser sources have been reported, which based on the femtosecond laser written waveguides in ZBLAN glass [33], Cr:ZnS [34], and Cr:ZnSe [35] crystals.

In this work, we report on the realization of Type I waveguides and 3D beam splitters at the wavelength of 4 μm in BGO crystal produced by direct femtosecond laser writing.

2. Experiments

An amplified Ti:Sapphire laser system, which produced linearly polarized pulses (120 fs duration, 800 nm wavelength, 1 mJ maximum energy, and a repetition rate 1 kHz) was utilized to fabricate straight waveguides and beam splitters in a BGO crystal with dimensions of 10 × 10 × 2 mm^3. In order to fabricate 3D structures with designed dimensions for MIR guiding, the multiscan procedure was implemented which implies the inscription of several parallel lines nearly overlapped. A 40 × microscope objective (N.A. = 0.40) was used to focus the beam approximately 50 μm below the largest surface of the crystal, that was positioned and moved with a XYZ translation stage. The scanning velocity was set to 500 μm/s in order to get an optimum spatial overlap between two consecutive pulses while minimizing the processing time as much as possible. Figure 1(a) shows a schematic of the femtosecond laser writing process. Many different trials were done changing the separation between adjacent tracks and pulse energy. Finally, the pulse energy (irradiated on the sample) of ~0.14 μJ and the separation of 3 μm were found as the best parameters, under our experimental conditions, for light guiding at 4 μm. In these conditions, two straight waveguides with 6 and 24 parallel scans, No. 1 and No. 2 respectively, were fabricated (see Fig. 1(b), left column). The 1 × 2 splitter (No. 3) was designed with a straight 3 mm length input arm, and two output arms with 0.4° of divergence (50 μm of lateral separation) at the same depth of the sample. The 1 × 3 splitter (No. 4) has a similar design and dimensions but the three outputs lie at different depths of the sample in a 3D configuration. Two 1 × 4 splitters were also implemented with lateral

#226064 - $15.00 USD Received 30 Oct 2014; revised 27 Nov 2014; accepted 28 Nov 2014; published 10 Dec 2014

separation between the arms of 60 and 110 μm (No. 5 and 6 respectively), forming squared 2 × 2 waveguide arrays at the output with 0.5° and 0.9° of divergence.

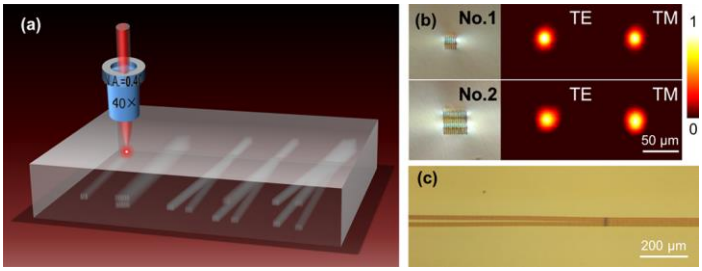

Fig. 1. (a) Schematic of the direct femtosecond laser writing process. (b) Optical microscope images of the cross sections of multiscan waveguides No. 1 (top) and No. 2 (bottom), and measured near-field intensity distributions at 4 μm. (c) Optical microscope image of the splitting point of the 1 × 4 beam splitter No. 6.

After direct femtosecond laser writing, the end faces were optically polished for measuring the guiding properties of the waveguides and beam splitters, resulting in a final length of 9.9 mm for all the waveguides. The microscope images of the cladding waveguide cross sections were taken by using a metalloscope (Axio Imager, Carl Zeiss) operating in transmission mode. The near-field modal distributions were investigated by utilizing a typical end-face arrangement. The linearly polarized laser at 4 μm, generated by the Tunable Laser System - MIRTM 8025 (Daylight Solutions, Inc.), was coupled into and out of the waveguides by MIR microscope objective lenses (ZnSe, LFO-5-12-3.75, N.A. = 0.13). A linear polarizer was placed before the input microscope objective lens to change the polarization of the incident light. Afterwards, a MIR beam imaging camera (WinCamD, DataRay Inc.) was employed to record the data. Based on the above arrangement and power meter, the propagation losses were determined by directly measuring the light powers coupled into and out of the end-faces. The coupling efficiency was estimated by considering the overlap of the incident light beam and waveguide mode. The coupling and Fresnel reflection losses of the waveguide systems were calculated as well.

3. Results and discussion

As shown in Fig. 1(b), the optical microscope images of the cross sections of the straight waveguides No. 1 and No. 2 exhibit well-defined rectangular shapes with dimensions of 16.4 × 18.3 μm^2 and 32.2 × 37.0 μm^2, respectively. Utilizing the multiscan technique, the desired waveguide cross sections were achieved with great precision and flexibility. In our previous work [23], Type II dual-line waveguides and depressed cladding waveguides were fabricated using the same laser facility but with different irradiation parameters. While for the dual-line waveguides, the pulsed energies were set to 1.68/2.52 μJ and the scan velocity was 50 μm/s, the parameters of the circular cladding waveguide was set to 1.68 μJ and 500 μm/s. In this work, in order to obtain waveguides for MIR with positive refractive index changes ($\Delta n > 0$) in the writing regions, the optimum parameters were found to be 0.14 μJ, 500 μm/s and 3 μm of lateral separation between tracks. As shown in Fig. 1(b), the Type I waveguides No. 1 and No. 2 supported fundamental mode guiding at 4 μm for both the TE and TM polarizations, respectively. By contrast, Type I waveguides in crystals reported before only supported guidance along one particular polarization direction [19,22].

The good performance of the straight waveguides reported above was also found in the beam-splitters (Nos. 3-6) that were written directly inside the BGO crystal with the same irradiation parameters. Figure 1(c) depicts the top view of the splitting point of beam splitter No. 6, showing smooth transition. The darker area around that point is produced by the irradiation with a larger amount of pulses as it is a stopping and starting point for the stage motion. The 1 × 2 and 1 × 3 splitters (Nos. 3 and 4) were fabricated with a 6 laser scans homogeneous section along all the waveguide (like waveguide No. 1), both in the entrance

#226064 - $15.00 USD Received 30 Oct 2014; revised 27 Nov 2014; accepted 28 Nov 2014; published 10 Dec 2014

waveguide as in the splitting arms. However, in splitters Nos. 5 and 6 the entrance waveguide was implemented with 24 scans (like waveguide No. 2) while the splitting arms have just 6 scans. We have used this strategy to decrease the laser damage at the splitting point and to obtain a more efficient beam division, making use of the fact that waveguides with both sections (Nos. 1 and 2) show similar fundamental mode performance. Figure 2 shows the microscope images of the end faces of the 1 × 2, 1 × 3, and 1 × 4 beam splitters. Also shown are the near-field intensity distributions of the beam splitters which, as expected, exhibit fundamental mode propagation at 4 μm along both the TE and TM polarizations.

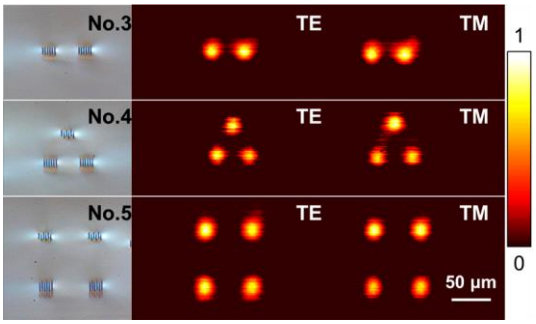

Fig. 2. Optical microscope images of the cross sections (left) and measured near-field intensity distributions at 4 μm of beam splitters Nos. 3-5 (right).

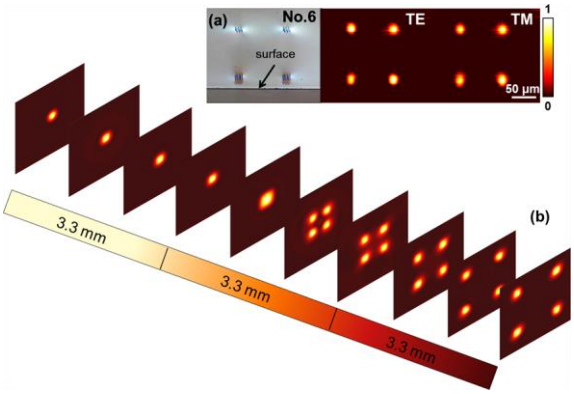

Fig. 3. (a) Optical microscope image of the cross section and measured near-field intensity distributions at 4 μm of the 1 × 4 beam splitter No. 6. (b) Simulated beam profile evolution for the 4 μm TE polarized light propagating along beam splitter No. 6.

In order to reconstruct the profile of the increased refractive index in the modified regions, we used the method introduced by Siebenmorgen *et al*. [36]. The calculated maximum refractive index contrast was estimated to be $(5.3 \pm 1) \times 10^{-3}$ for BGO straight waveguides at 4 μm. It seems reasonable to assume that the refractive index changes at 4 μm are approximately the same for the beam splitters. We simulated the light propagation at 4 μm by using the commercial program BeamPROP (Rsoft©, Inc), which is based on the finite-difference beam propagation method (FD-BPM) [37]. To determine more accurately the magnitude of the refractive index change (Δn), the same waveguide design was tested in the software with different values of Δn, ranging from 4.3×10^{-3} to 6.3×10^{-3} in 0.1×10^{-3} steps. By comparing the simulated profiles with the measured near-field intensity distribution in Fig. 3(a), the refractive index changes of the waveguide was determined to be 5.0×10^{-3}, for which the best agreement with the experimental results was obtained. Figure 3(b) shows the simulated beam profile evolution of 4 μm light propagating on TE polarization along the 1 × 4 beam splitter No. 6. As depicted in Fig. 3(a), a clear beam splitting is observed at the waveguide output with measured intensity splitting ratio of 27:26:23:24 for the four arms.

#226064 - $15.00 USD Received 30 Oct 2014; revised 27 Nov 2014; accepted 28 Nov 2014; published 10 Dec 2014

Although the splitting ratio is not equal, it could be improved by optimizing the design and processing parameters.

Table 1. Propagation Losses α (dB/cm) of the BGO Waveguides and Beam Splitters

	No. 1	No. 2	No. 3	No. 4	No. 5	No. 6
TE	3.39	3.70	3.35	3.70	3.81	3.95
TM	3.22	3.47	3.23	3.47	3.59	3.71

Table 1 shows the propagation losses (α) of the femtosecond laser writing waveguides and beam splitters (the coupling loss (~0.97 dB) and Fresnel reflection loss of the two end faces (:1.07 dB) are not included in the propagation loss). As one can see, the differences between TE and TM polarizations were less than 7%, showing the good features of polarization-insensitive guidance. The all-angle light transmission to investigate the thorough information of the polarization effects of the guidance was shown in Fig. 4. It is found that the guidance exists for the 4 μm laser light at any transverse polarizations. By comparing the propagation losses of the straight waveguides and beam splitters written with the same parameters, the additional losses of the 3D splitters were determined to be less than ~0.3 dB. A part of the splitting losses could be attributed to the imperfections of the structures, but the obtained values are significantly smaller than those reported for femtosecond laser written 1 × 3 splitters in pure fused silica (the splitting losses ~6 dB) [10].

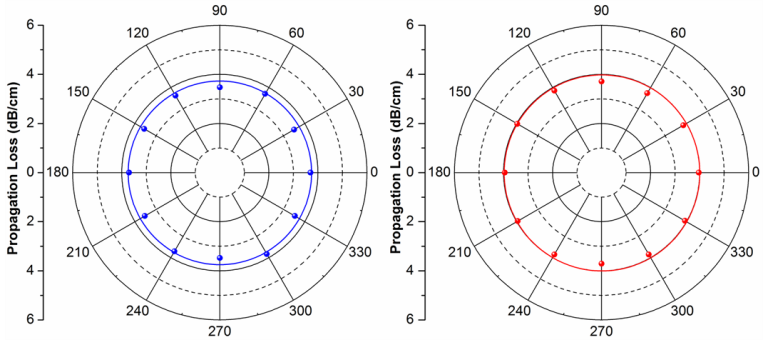

Fig. 4. Polar images of the propagation losses of BGO waveguide No.2 (a) and beam splitter No.6 (b) measured at 4 μm.

4. Summary

In conclusion, we have demonstrated the fabrication of 3D beam splitters in BGO crystal by direct femtosecond laser writing. For the waveguides and beam splitters with positive refractive index changes, fundamental mode guidance are achieved along both TE and TM polarizations at the wavelength of 4 μm. The propagation losses and splitting losses are estimated to be less than 4 dB/cm and 0.3 dB respectively, and the splitting ratio is almost equalized. The results show the promising capability of direct femtosecond laser written complex devices in BGO crystal for MIR applications.

Acknowledgments

This work was supported by the National Natural Science Foundation of China (No. 11274203), Junta de Castilla y León under project (SA086A12-2), and Ministerio de Economía y Competitividad under project (FIS2013-44174-P), Spain.

#226064 - $15.00 USD Received 30 Oct 2014; revised 27 Nov 2014; accepted 28 Nov 2014; published 10 Dec 2014